Article:
Acomb, JC, Wu, C and Williams, PT (2015) Effect of growth temperature and feedstock:catalyst ratio on the production of carbon nanotubes and hydrogen from the pyrolysis of waste plastics. Journal of Analytical and Applied Pyrolysis, 113. 231 - 238. ISSN 0165-2370

https://doi.org/10.1016/j.jaap.2015.01.012

Effect of growth temperature and feedstock:catalyst ratio on the production of carbon nanotubes and hydrogen from the pyrolysis of waste plastics

Jonathan C. Acomb[a], Chunfei Wu[a,b] and Paul T. Williams[a*]

[a] Energy Research Institute, The University of Leeds, Leeds LS2 9JT, UK.
(Tel: +44 113 3432504; Email: p.t.williams@leeds.ac.uk)
[b] School of Engineering, University of Hull, Hull, HU6 7RX, UK

Abstract

Carbon nanotubes have been produced from a low density polyethylene (LDPE) feedstock via a two stage pyrolysis process. The temperature of the second stage, where carbon deposition on an iron alumina catalyst occurs (growth temperature), was varied using catalyst temperatures of 700, 800 and 900 °C. An increase in catalyst temperature led to a higher yield of both carbon nanotubes and hydrogen, as the rate of carbon deposition increased. Changing the amount of feedstock relative to the catalyst also had an effect on the production of both carbon nanotubes and hydrogen. As more feedstock is used a larger source of carbon gives rise to a larger amount of carbon nanotubes per gram of catalyst. However, in terms of the percentage of feedstock converted into carbon nanotubes and hydrogen gas, a reduction was observed. Conversion of plastic into carbon nanotubes was 29.1 wt.% when 0.5g LDPE was used, but reduced to 13.1 wt.% with 1.25g LDPE. This is because the catalyst activity reduces as it becomes overloaded, and much of the hydrocarbon gases are left unreacted. This gives an economic playoff between large conversion of plastics into carbon nanotubes and hydrogen gas, and large yields of carbon nanotubes per gram of catalyst used.

Keywords: Plastics; Carbon nanotubes; Catalyst; Hydrogen

Introduction

Carbon nanotubes (CNTs) are high value materials which have generated a great deal of research interest in recent years as they have potential uses in a wide range of applications [1-8]. This stems from their remarkable properties including high strength, a large surface area and good electrical conductivity [9]. Whilst they were first produced by Ijima et al by an arc discharge process [10], large scale production favours chemical vapour deposition of hydrocarbon gases such as methane and acetylene. In more recent years a method of producing carbon nanotubes from the pyrolysis of plastics has been demonstrated [11-21]. This has the benefit of producing valuable products from a waste resource, whilst simultaneously tackling the waste management issues associated with waste plastics, which are often difficult to recycle.

Production of carbon nanotubes from the pyrolysis of plastics works in a similar manner to chemical vapour deposition, with the pyrolysis gases depositing onto the surface of a catalyst. Whilst nickel catalysts are often utilised in thermal treatment for the production of liquids and gases [22-28], iron catalysts are more often used for carbon nanotube production [29-35]. This is because when directly compared with nickel catalysts, iron has been found to produce a larger yield of CNTs [29, 31, 33, 35].

Production of carbon nanotubes from virgin plastics was demonstrated by Kukovitsky et al [16], where polyethylene was pyrolysed with a nickel plate catalyst at 450 °C. Crooked carbon nanotubes were produced along with other filamentous carbons. Subsequent studies by Kukovitsky and other research groups [11-13, 15-19, 21] obtained large yields of CNTs through pyrolysis of virgin plastics using higher reaction temperatures of up to 900 °C. Pyrolysis of real world waste plastics have also been used to generate carbon nanotubes, with studies making use of waste polypropylene and polyethylene [20, 36, 37].

If a two stage pyrolysis process is employed, a large yield of carbon nanotubes and hydrogen gas can be produced simultaneously [11, 19, 37]. Hydrogen gas is an important alternative fuel that could play a key role in future energy needs. It is considered a green alternative to fossil fuels since its combustion gives off no carbon dioxide. Its production from thermal treatment of plastics is well established, with steam gasification proving a fruitful means of achieving large hydrogen yields [23, 28, 38-42]. However in previous research by this research group it was found that whilst giving larger yields of hydrogen, adding steam to the thermal treatment of LDPE leads to a reduction in CNT yields [11]. The research used a two stage process where evolved pyrolysis gases are passed directly onto the second stage, producing large amounts of carbon nanotubes and hydrogen gas [11, 37]. Liu et al [19] also used a two stage pyrolysis process where plastics are pyrolysed in a first stage and the gases separated and passed to a second stage where carbon nanotubes and hydrogen gas were produced using a nickel catalyst.

In order to optimise production of carbon nanotubes and hydrogen, different parameters can be varied. The temperature used for the growth of carbon nanotubes is a crucial factor in chemical vapour deposition, and has an effect on the growth rate [43-46]. Lee et al [46] used a series of growth temperatures between 750 and 950 °C with an iron catalyst and found that the growth rate of carbon nanotubes increased with growth temperature. Whilst there are differing views on the effect of temperature, Lee et al proposed that increased growth rate occurred as a result of faster carbon diffusion through the catalyst particles. This is an important step in the growth of carbon nanotubes, and is considered by some to be the rate determining step [47]. Similar results were also obtained when plastic was used as the feedstock. Liu et al [19] found that increasing the decomposition temperature between 500 °C and 700 °C increased the yield of carbon nanotubes obtained, with a small dip in production tha that observed at 800 °C. In terms of hydrogen production, a number of studies have found

that raising the reaction temperature tends to result in an increase in the hydrogen yield obtained, as more hydrocarbons decompose [19, 38, 48, 49]. When hydrogen and carbon nanotubes are produced simultaneously, increasing the temperature sees an increase in the yields of both, since hydrogen is produced during carbon deposition [19, 50].

Another key factor in the production of carbon nanotubes is the amount of feedstock relative to the amount of catalyst used. A number of studies have shown that during thermal treatment of hydrocarbons, the catalytic activity of a catalyst reduces with decreasing catalyst weight [51-53]. In terms of carbon nanotube production, Das et al [44] varied the amount of iron catalyst compared to various liquid hydrocarbon feedstocks, and found that with a lower catalyst:feedstock ratio less CNTs were produced.

This work has considered the effect of growth (catalyst) temperature and the amount of feedstock used on the production of carbon nanotubes and hydrogen from a low density polyethylene feedstock using an iron catalyst. In addition, the amount of feedstock used was varied in relation to the mass of catalyst, which was kept constant, so that the effect of changing the ratio of feedstock:catalyst could be investigated.

Materials and methods

Low density polyethylene (LDPE) was obtained from ACROS Organics UK. An iron catalyst was prepared by impregnation onto an alumina support, with an iron loading of 10 wt.%. $Fe(NO_3)_3 \cdot 9H_2O$, and gamma Al_2O_3 were used as the raw materials. Iron nitrate was dissolved in ethanol, following which the alumina was added and the mixture left until it formed a slurry. This was then dried overnight in an oven at 50 °C to remove the remaining ethanol before calcination to a temperature of 750 °C at a heating rate of 2 °C min^{-1} in an air

atmosphere with a hold time of 3h. The catalysts were then crushed and sieved to give granules of between 0.065 and 0.212 mm.

The experimental system consisted of a two-stage pyrolysis reactor as shown in Fig. 1. The reactor was made of stainless steel and had a total length of 320 mm and an internal diameter of 22 mm. Two sets of experiments were carried out, the first investigating the growth temperature and the second investigating the feedstock:catalyst ratio.

For the investigation of temperature 1 g of the LDPE was placed inside a sample boat and pyrolysed in the first reactor, where the temperature was heated to 600 °C. The generated gaseous products were then passed through to the second reactor and passed over 0.5 g of catalyst allowing carbon deposition to occur on the catalyst surface. The temperature of this second reactor where the catalyst was pre-heated and held at 700, 800 or 900 °C. Nitrogen was used as the carrier gas with a flow rate of 80 ml min^{-1}. The procedure was to heat the second gasification reactor to the desired temperature, then heat the first reactor to 600 °C at a heating rate of 50 °C min^{-1} for a total reaction time of 30 min.

For the investigation of the sample to catalyst ratio the same procedure was carried out, except in this case the temperature of the second reactor was 800 °C for all experiments, whilst the variable in this case was the amount of LDPE sample used. This was varied between, 0.5, 0.75, 1.0 and 1.25g, with the amount of iron catalyst held constant at a value of 0.5g.

The volatile products after the gasification process were passed through two dry-ice cooled condensers, where any condensed products were collected. The non-condensed gases were collected in a 25 L Tedlar™ gas sample bag. The reproducibility of the reaction system was tested and experiments were repeated to ensure the reliability of research results.

The gases collected in the gas sample bag were analysed by packed column gas chromatography (GC). Hydrocarbons (C_1–C_4) were analysed using a Varian 3380 gas chromatograph with a flame ionisation detector, with an 80–100 mesh Hysep column and nitrogen carrier gas. Permanent gases (H_2, CO, O_2, N_2 and CO_2) were analysed with a separate Varian 3380 GC/TCD, thermal conductivity detector, with two packed columns. A 2 m long and 2 mm diameter column packed with 60–80 mesh molecular sieve was used to analyse hydrogen, nitrogen, carbon monoxide and oxygen. Carbon dioxide was analysed on a 2 m long and 2 mm diameter column with Haysep 60–80 mesh molecular sieve. The carrier gas was argon.

Carbon deposition on the catalyst was analysed by a range of techniques. High resolution scanning and transmission electron microscopy was undertaken using a SEM, LEO 1530 and TEM, FEI Tecnai TF20, to characterise the nature of the carbon that was deposited on the surface of the catalysts during the experimental procedure. The reacted catalysts were analysed by temperature programmed oxidation to investigate the types and relative amounts of carbon deposits on their surfaces. Around 20 mg of the reacted catalyst was heated in a thermogravimetric analyser in an atmosphere of air at a heating rate of 15 °C min^{-1}up to a temperature of 800 °C and with a hold time of 10 min. Raman spectroscopy was undertaken on the carbon deposits on the catalyst surface to determine their graphitic quality. Results were obtained using a Renishaw Invia Raman spectrometer at a wavelength of 514 nm at Raman shifts between 100 and 3200 cm^{-1}.

Results and discussion

1.1 Effect of temperature

1.1.1 Mass balance and hydrogen production

Figures 2(a) and (b) show the mass balances and gas compositions of the experiments at 700, 800 and 900 °C catalyst temperature. Mass balances are reported in terms of solids, liquids and gases produced, where the solids account for the carbon deposition on the catalyst surface. All mass balances obtained were above 89 wt.%. As the reaction temperature was raised, the amount of solids produced rises, showing that more carbon deposition occurs. This is consistent with a number of studies, which see an increase in carbon deposition at higher temperatures [43-46]. The yield of gases initially increases with temperature as the larger hydrocarbons are broken down into gases, consistent with the reduction in liquids observed. At 900 °C however a reduction in the yield of gases occurs. At this temperature more of the gases are converted into solid carbons on the surface of the catalyst, via equation 1, accounting for the increase in solids seen at this temperature.

Equation 1: $C_xH_y \xrightarrow[Iron\ catalyst]{} C + H_2$

In terms of the gas composition it can be seen from Figure 2(b) that with increasing temperature the amount of hydrogen increases. This is also shown in Figure 2(c) which shows the amount of hydrogen produced as a percentage of the maximum theoretical yield obtainable. The maximum theoretical yield was calculated based on the total amount of hydrogen in the plastic as obtained from elemental analysis. As the amount of solid carbons produced increases, the amount of hydrogen produced also increases, since both are produced during the decomposition of hydrocarbons via equation 1. This is consistent with other studies investigating the production of hydrogen and carbon nanotubes [19, 50]. Figure 2(b)

shows that the composition of C_2-C_4 hydrocarbons reduce as the temperature is raised as they are either broken down to form methane, or deposited on the catalyst to form solid carbons.

1.1.2 Carbon nanotube production

Scanning and transmission electron microscopy were undertaken on the carbon deposition on the catalyst surface, with the images obtained shown in Figures 3(a-f). The SEM image of the catalyst obtained at 700 °C catalyst (growth) temperature, Figure 3(a) shows the presence of filamentous carbons, as well as accumulations of more amorphous and encapsulating carbon. The corresponding TEM image Figure 3(d) confirmed that the filamentous carbons were multiwalled carbon nanotubes, which had diameters of around 20-30 nm and were up to a number of micron in length. The amorphous and encapsulating carbons observed using SEM are also seen, and could contribute to the low yield of hydrogen at this temperature by deactivation of the catalyst. The deposits on the surface of the catalyst obtained from 800 °C also show the presence of filamentous carbons on their SEM image in Figure 3(b), however in this case they are far more densely packed and show no visible amorphous carbons. This is in accordance with a study by Mishra et al [20] who likewise saw a reduction of amorphous type carbon deposition with an increase in temperature up to 800 °C, when compared with temperatures of 600 and 700 °C. The corresponding TEM image for the carbon deposits obtained at 800 °C in Figure 3(e) confirms that the filamentous carbons are multiwalled carbon nanotubes, with dimensions similar to those seen at 700 °C, with diameters of around 20-30 nm and lengths of up to several micron. Thick deposits of filamentous carbons are also seen on the SEM image for the carbon deposition on the catalyst obtained from 900 °C in Figure 3(c), however the TEM image in Figure 3(f) shows that the quality of the carbon nanotubes has deteriorated. The filamentous carbons no longer show continuous and even walls, with some showing no hollow inner channel at all. The diameters of the filamentous

carbons also increased to widths of 30-60 nm, with the lengths similar to those produced at other temperatures, being a number of micron..

Raman spectroscopy is often used to characterise CNTs [13, 54-57], and was also undertaken in this study to characterise the carbon deposits produced, with the resultant Raman spectra for 700, 800 and 900 °C shown in Figure 4. Peaks are seen at 1589 and 1348 cm^{-1} wavelength for each of the samples. The peak at 1589 cm^{-1} corresponds to the G peak associated with graphitic carbon within the sample, the peak at 1348 cm^{-1} corresponds with the D peak and is associated with defects within the graphitic lattice; while the G' peak at the Raman shift around wavelength 2709 cm^{-1} indicates the two photon elastic scattering process, indicating the purity of CNTs. The ratio between the size of the G peak and D peak is a useful way of comparing the quality of the carbon nanotubes obtained in terms of how ordered and graphitic they are [14, 50, 58, 59]. This will enable the purity of the deposits in terms of the carbon nanotubes produced to be evaluated, with a larger G/D ratio indicating a higher purity. The Raman spectra shown in Figure 4 show that the G/D ratio is significantly lower for a catalyst temperature of 700 °C, with a value of 1.66, than for the catalyst temperatures of 800 and 900 °C with values of 1.97 and 1.93 respectively. This indicates that the carbon deposition at this lower temperature has a lower purity in terms of carbon nanotubes, as seen by electron microscopy. In addition, the CNTs produced at 700 °C also show the lowest intensity ratio of G'/G, compared to the CNTs produced at other temperatures; this further supports that CNTs produced at such low temperature (700 ˚C) have the lowest purity. Mishra et al [20] likewise obtained a higher G/D ratio for carbon deposits obtained from higher reaction temperatures, indicating a higher quality of carbon nanotubes. A slight reduction in the G/D ratio is seen at 900 °C, and is most likely due to the fact that despite

there being more carbon deposition, the quality of the filamentous carbon is lower, with less ordered carbon walls, as observed from TEM.

In order to better determine the amount of carbon deposition and the relative amounts of carbon types on the catalyst surface, temperature programmed oxidation (TPO) was carried out on the used catalyst samples. The derivative TPO plots in Fig. 5(a) show two distinct peaks, one between 350 °C and 450 °C, and another between 500 °C and 700 °C. Amorphous carbons are reported to show a peak at lower temperatures than filamentous carbons, due to their more reactive nature [60]. As such, the lower temperature TPO peak is associated with the oxidation of amorphous carbons whilst the high temperature TPO peak is associated with the oxidation of filamentous carbons such as carbon nanotubes.

Using the derivative TPO plot the total amount of each carbon type was calculated and displayed in Figure 5(b). As the temperature is raised, the amount of filamentous carbons produced increases, with 213 mg produced at 900 °C compared with 20mg and 179mg at 700°C and 800 °C respectively. The percentage of plastic converted into CNTs was calculated based on the weight of carbon nanotubes produced as a percentage of the weight of LDPE used. These results show that more of the plastic is converted into carbon nanotubes as the temperature is increased, as can also be seen in Figure 5(b). This is in accordance with other studies [43-46], and is likely to be due to the increase in the diffusion rate of carbon through the catalyst particle, an important step in the formation of carbon nanotubes. The amount of amorphous carbon produced at a catalyst temperature of 700 °C is also significantly more than that produced at the other temperatures, with a further reduction also seen between catalyst temperatures of 800 °C and 900 °C. This shows that an increase in temperature also favours the production of CNTs over amorphous carbons.

Whilst more carbon deposition was produced at 900 °C, the TEM images and Raman spectroscopy showed that the quality of the carbon nanotubes in terms of the crystallinity and order of the walls produced at the catalyst temperature of 800°C was higher. CNTs produced at 800 °C showed similar dimensions to those produced from more standard methods such as chemical vapour deposition, with comparable Raman spectra results in terms of G:D ratio also obtained [50, 61, 62]. This opens up the possibility of using the CNTs obtained in commercial applications. Multiwalled CNTs find current uses in a range of applications ranging from high strength composites, coatings, water treatment and energy technologies [63-70]. In order to be used in these applications however, a purification process would need to be undertaken on the CNTs to separate the carbons from the catalyst and to remove amorphous carbons and other contaminants.

1.2 Effect of feedstock:catalyst ratio

1.2.1 Mass balance and hydrogen production

Figure 6 shows the results for the mass balance and gas composition for experiments where the feedstock:catalyst ratio was varied, by changing the amount of LDPE used. From Figure 6(a) it can be seen that as the amount of plastic used is increased, the percentage converted into solids reduces, whilst the percentage of gases and liquids increases. This is because when more of the feedstock is used, the catalyst starts to get overloaded. The result is that not all the pyrolysis gases can gain access to the catalyst surface to react and deposit as carbon, yielding fewer solids. This also leads to a larger amount of longer hydrocarbons since they are left unreacted. This is mirrored in the gas composition shown in Figure 6(b), as the amount of C_2-C_4 hydrocarbons rises as the amount of LDPE used increases, since it was unable to react with the overloaded catalyst. This is consistent with other studies based on hydrocarbon gasification which show that the catalytic activity of a catalyst reduces with decreasing catalyst weight [51-53].

The percentage of hydrogen produced in the gases also reduces with more feedstock used, since a smaller proportion of the feedstock is converted into hydrogen and carbon via equation 1 as a result of reduced catalytic activity. This is also shown in Figure 6(c) where a reduction observed in the percentage of hydrogen in the plastic converted into hydrogen gas. Other studies on hydrogen production from hydrocarbon sources have also found similar results, with hydrogen production reducing as the amount of catalyst relative to the feedstock is lowered [51-53, 71].

1.2.2 Carbon nanotube production

The carbon deposits produced from different amounts of plastic were analysed by SEM and TEM (not shown here), but showed little variation in the images obtained.

TPO of the carbon on the used catalyst was undertaken to determine the amount of different types of carbon deposition. Figure 7(a) shows the derivative TPO thermograms obtained, and similar to the TPO results shown in Figure 5(a) also shows the two distinct peaks associated with amorphous carbons, 350 – 450 °C, and filamentous carbons 500 – 700 °C. The higher temperature filamentous TPO peak is significantly larger for all the experiments, as expected, based on the results obtained for the catalyst temperature of 800 °C. From the derivative TPO thermogram the amounts of amorphous and filamentous carbons produced were calculated and are shown in Figure 7(b). As the amount of feedstock used increases, the amount of carbon nanotubes obtained increases from 146 mg at 0.5g LDPE up to 179 mg at 1.0g LDPE. This is expected as there is a larger source of carbon when more LDPE is used. Das et al [44] found similar results when producing carbon nanotubes from liquid hydrocarbons. A higher yield of wt CNT/wt catalyst, was obtained at low catalyst:carbon ratios, when more feedstock is used relative to the amount of catalyst. The increase in CNT yield is shown up to 1.25g of LDPE, where a slight reduction (164mg) in the amount of CNTs is observed. At the amount of 1.25 g LDPE a larger amount of amorphous carbons were produced. Unlike filamentous

carbons such as carbon nanotubes, amorphous carbons are known to deactivate the catalyst by encapsulating catalyst particles [72], preventing the production of CNTs and hydrogen.

Though more CNTs are produced with higher usage of LDPE, the percentage conversion of the plastic into carbon nanotubes, shown in Figure 7(b), reduces. When 0.5 g of LDPE is used 29.1 wt.% of the plastic is converted into carbon nanotubes, but when 1.25g of sample is used, only 13.1 wt.% of the plastic is converted. This is in accordance with the mass balance results, as access to the catalyst becomes lower as the catalyst becomes overloaded and pyrolysis gases are unreacted, producing a lower catalyst activity. When the feedstock:catalyst ratio is low, i.e. a small amount of plastic is used, the conversion of the plastics is high, however the amount of CNTs compared to the amount of catalyst used is low. The opposite is found at higher feedstock:catalyst ratios, with lower plastic to CNT conversions, but a larger amount of CNT production compared to the amount of catalyst. This sets up an interesting economic playoff between achieving high plastic conversions and the amount of catalyst used per gram of CNTs produced. In order for the process to become economic however, the current batch method would need to be modified to a continuous process. This could be achieved by using similar conditions and materials in a two stage process using a screw kiln for the first stage and where the second stage is replaced by a moving bed or screw kiln reactor where the catalyst could be collected after use followed by separation and purification of the product CNTs.

Conclusions

A two-stage pyrolysis-catalytic reactor has been used to produce hydrogen and carbon nanotubes from waste plastic (low density polyethylene). Carbon nanotubes are formed through decomposition of hydrocarbons derived from the pyrolysis of the plastic on a catalyst

surface, producing solid carbons as well as hydrogen gas. Carbon deposition increased with catalyst reaction temperature, with a larger amount of CNTs produced at higher temperatures. This was because the growth rate of CNTs increases with reaction temperature as a result of faster carbon diffusion through the catalyst particle. This is thought to be the rate determining step in CNT formation, and so its increase leads to a larger CNT yield. Hydrogen production increases with the increase in CNTs production, since the two are both produced simultaneously by the decomposition of hydrocarbons. The highest quality CNTs were produced at 800 °C, with 700 °C producing more amorphous carbons and 900 °C producing less uniform CNTs.

Increasing the amount of LPDE used increased the CNTs yield up to a certain level. At 1.25g LDPE loading, the yield of CNTs reduces due to the production of amorphous carbons. Whilst more carbon nanotubes were produced at higher LDPE loading, the percent conversion from plastics to CNTs reduced since the catalyst became overloaded and a large amount of pyrolysis gases were left unable to deposit on the catalyst surface. This gives an economic playoff between large conversion of plastics into CNTs and large yields of CNTs per gram of catalyst used.

Figure 1

Schematic diagram of the experimental reactor system.

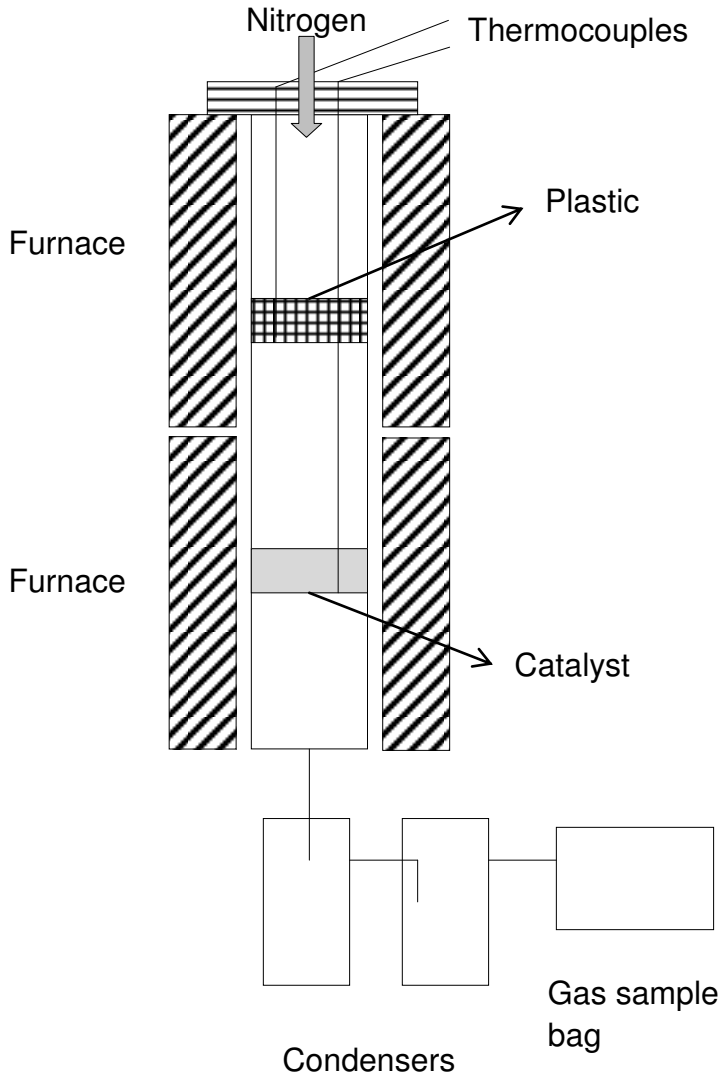

Figure 2

Effect of catalyst growth temperature on (a) mass balance, (b) gas composition and (c) hydrogen conversion from the two stage pyrolysis-catalysis of LDPE

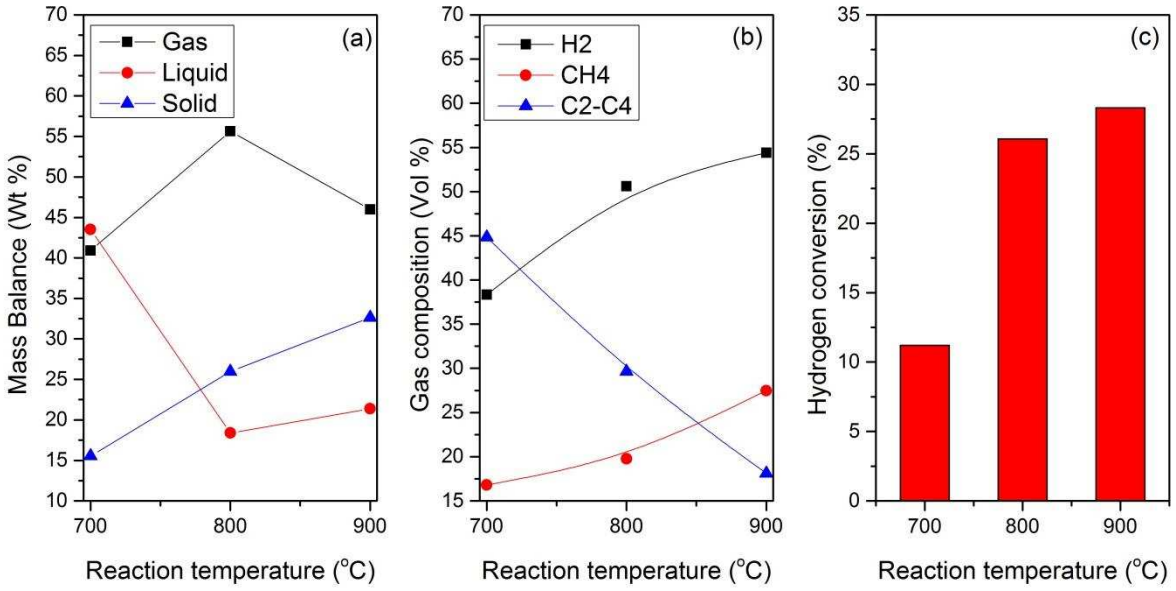

Figure 3

Scanning electron microscopy and transmission electron microscopy images of carbon deposition on the catalyst at catalyst (growth) temperatures of 700 °C (a) and (d), 800 °C (b) and (e) and 900°C (c) and (f) respectively.

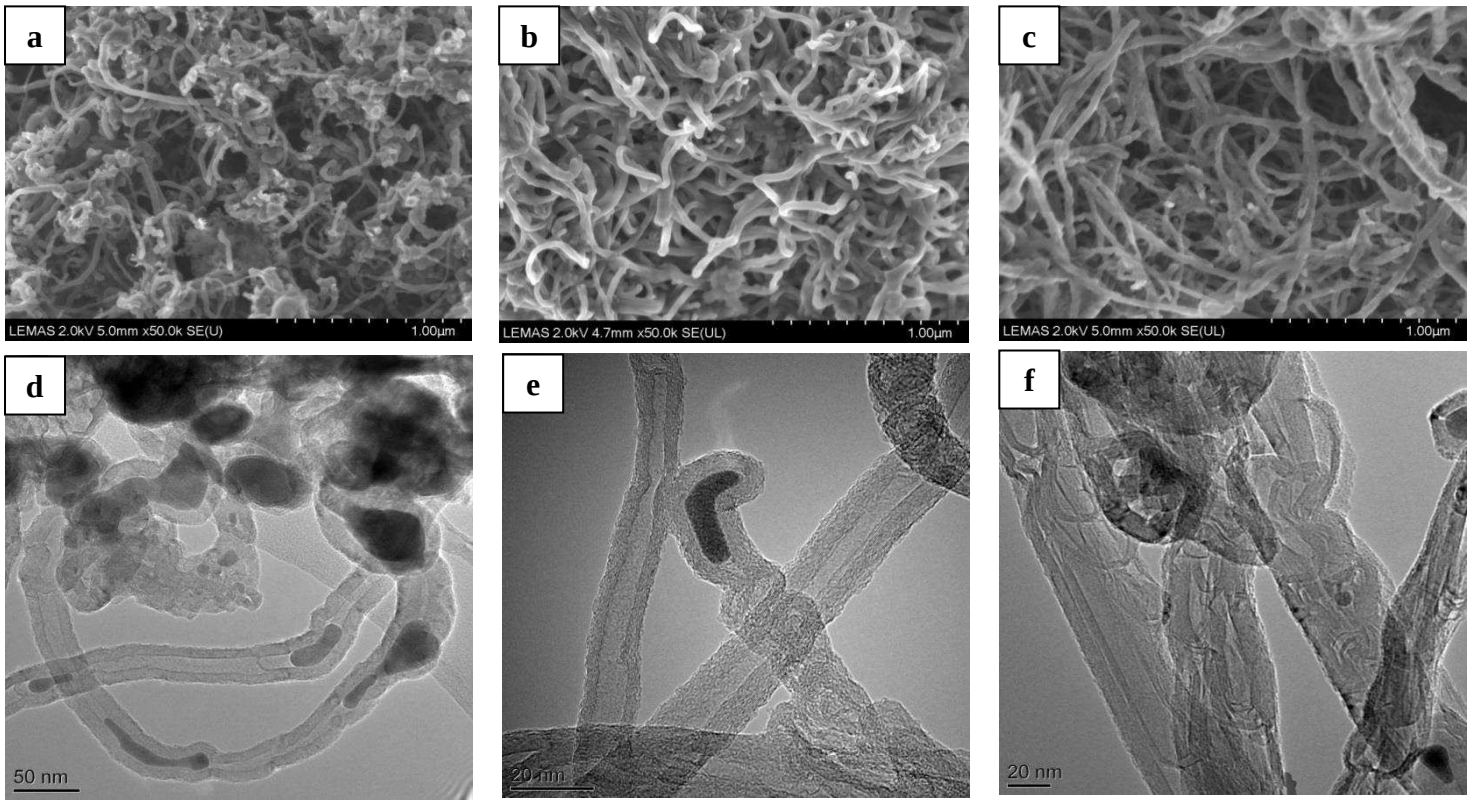

Figure 4

Raman spectra of carbon deposits obtained from catalyst temperatures of (a) 700 °C, (b) 800 °C and (c) 900 °C.

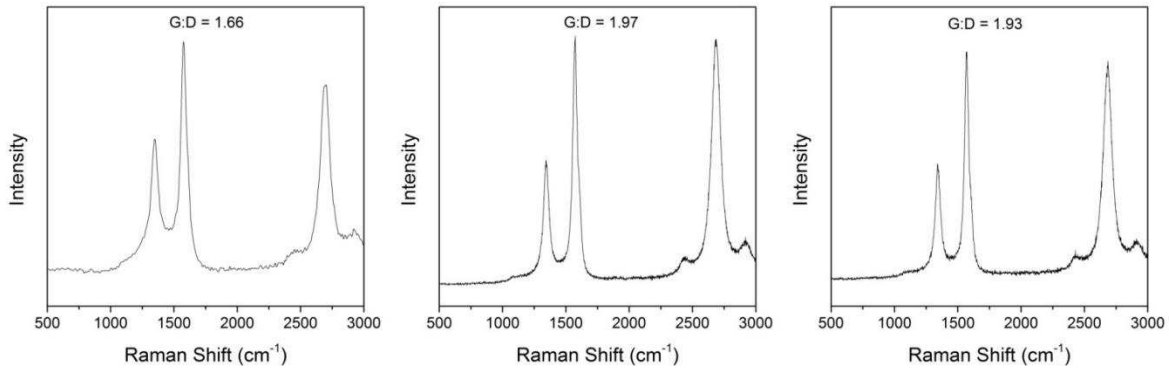

Figure 5

Temperature programmed oxidation (TPO) thermograms showing the effect of catalyst temperature; (a) derivative TPO thermograms and (b) amount of carbon deposition and conversion of plastic to CNTs

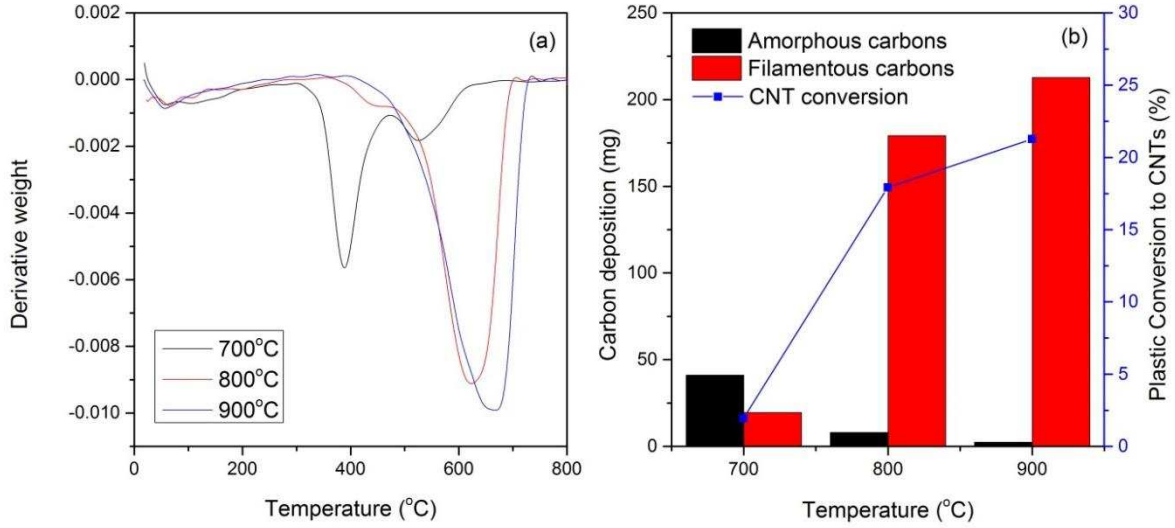

Figure 6

Effect of sample:catalyst ratio on (a) mass balance, (b) gas composition and (c) hydrogen conversion from the two stage pyrolysis-catalysis of LDPE

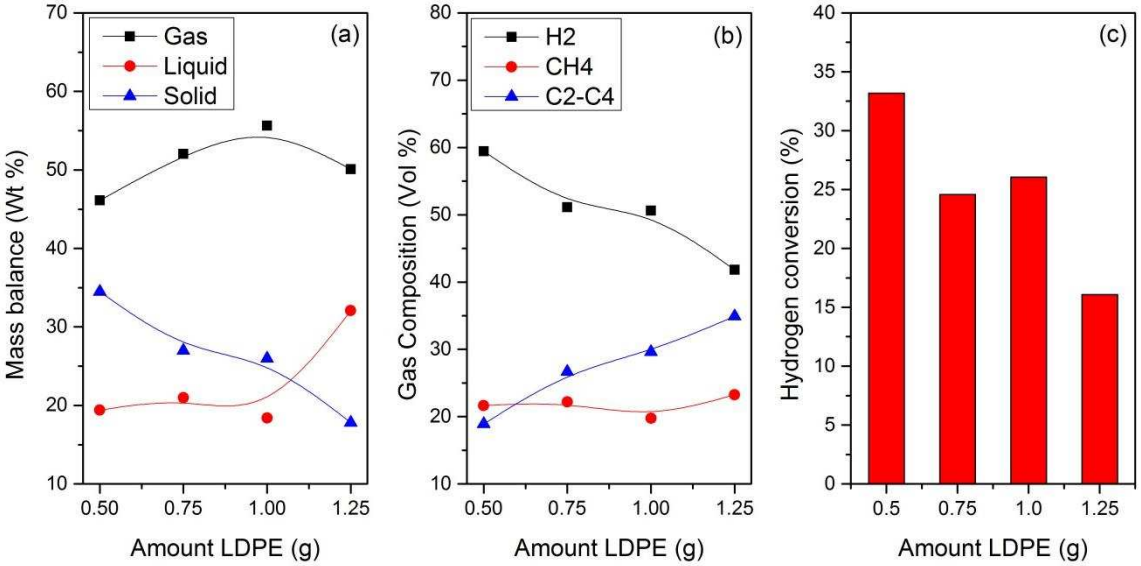

Figure 7

Temperature programmed oxidation thermograms showing effect of temperature; (a) derivative plot and (b) amount of carbon deposition and conversion of plastic to CNTs

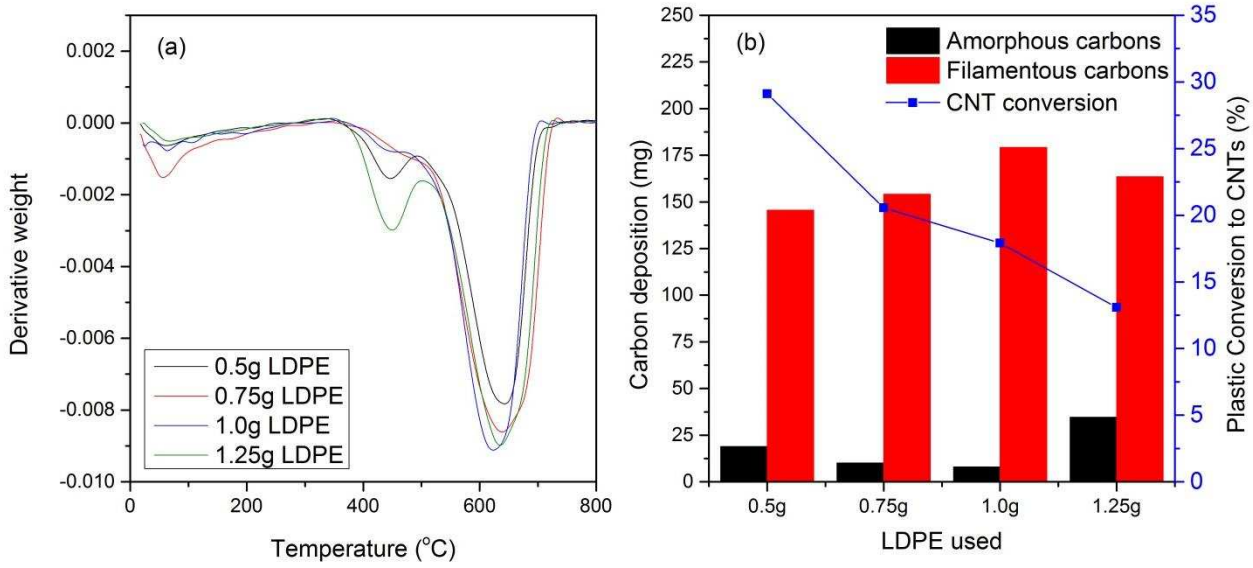

1. Ajayan, P.M., et al., Single-walled carbon nanotube-polymer composites: Strength and weakness. Advanced Materials, 2000. **12**: p. 750-753.
2. Hinds, B.J., et al., Aligned multiwalled carbon nanotube membranes. Science, 2004. **303**(5654): p. 62-5.
3. Javey, A., Ballistic carbon nanotube field-effect transitors. Nature, 2003. **424**: p. 654-657.
4. Kymakis, E., I. Alexandrou, and G.A.J. Amaratunga, High open-circuit voltage photovoltaic devices from carbon-nanotube-polymer composites. Journal of Applied Physics, 2003. **93**(3): p. 1764.
5. Li, W., et al., Carbon nanotubes as support for cathode catalyst of a direct methanol fuel cell. Carbon, 2002. **40**: p. 787-803.
6. Sae-Khow, O. and S. Mitra, Carbon Nanotube Immobilized Composite Hollow Fiber Membranes for Pervaporative Removal of Volatile Organics from Water. Journal of Physical Chemistry C, 2010. **114**: p. 16351–16356.
7. Shimoda, H., et al., Lithium Intercalation into Opened Single-Wall Carbon Nanotubes: Storage Capacity and Electronic Properties. Physical Review Letters, 2001. **88**(1).
8. Snow, E.S., et al., Chemical detection with a single-walled carbon nanotube capacitor. Science, 2005. **307**(5717): p. 1942-5.
9. Nessim, G.D., Properties, synthesis, and growth mechanisms of carbon nanotubes with special focus on thermal chemical vapor deposition. Nanoscale, 2010. **2**(8): p. 1306-23.
10. Iijima, S., Helical Microtubules of Graphitic Carbon. Letters to Nature, 1991. **354**: p. 56-58.
11. Acomb, J.C., C. Wu, and P.T. Williams, Control of steam input to the pyrolysis-gasification of waste plastics for improved production of hydrogen or carbon nanotubes. Applied Catalysis B: Environmental, 2014. **147**: p. 571-584.
12. Arena, U. and M.L. Mastellone, Production of Multi-wall Carbon Nanotubes by Means of Fluidized Bed Pyrolysis of Virgin or Recycled Polymers. European Nanosystems, 2005. **2005**.
13. Arena, U., et al., An innovative process for mass production of multi-wall carbon nanotubes by means of low-cost pyrolysis of polyolefins. Polymer Degradation and Stability, 2006. **91**(4): p. 763-768.
14. Arnaiz, N., et al., Production of Carbon Nanotubes from Polyethylene Pyrolysis Gas and Effect of Temperature. Industrial & Engineering Chemistry Research, 2013. **52**(42): p. 14847-14854.
15. Chung, Y.-H. and S. Jou, Carbon nanotubes from catalytic pyrolysis of polypropylene. Materials Chemistry and Physics, 2005. **92**(1): p. 256-259.
16. Kukovitskii, E.F., et al., Carbon nanotubes of polyethylene. Chemical Physics Letters, 1997. **266**: p. 323-328.
17. Kukovitsky, E.F., et al., CVD growth of carbon nanotube films on nickel substrates. Applied Surface Science, 2003. **215**(1-4): p. 201-208.

18. Kukovitsky, E.F., et al., Correlation between metal catalyst particle size and carbon nanotube growth. Chemical Physics Letters, 2002. **355**(5-6): p. 497-503.

19. Liu, J., et al., Catalytic pyrolysis of polypropylene to synthesize carbon nanotubes and hydrogen through a two-stage process. Polymer Degradation and Stability, 2011. **96**(10): p. 1711-1719.

20. Mishra, N., et al., Pyrolysis of waste polypropylene for the synthesis of carbon nanotubes. Journal of Analytical and Applied Pyrolysis, 2012. **94**: p. 91-98.

21. Zhang, J.H., et al., Synthesis and characterization of larger diameter carbon nanotubes from catalytic pyrolysis of polypropylene. Materials Letters, 2008. **62**(12-13): p. 1839-1842.

22. Aupretre, F., C. Descorme, and D. Duprez, Bio-ethanol catalytic steam reforming over supported metal catalysts. Catalysis Communications, 2002. **3**: p. 263-267.

23. Czernik, S. and R.J. French, Production of Hydrogen from Plastics by Pyrolysis and Catalytic Steam Reform. Energy & Fuels, 2006. **20**: p. 754-758.

24. French, R. and S. Czernik, Catalytic pyrolysis of biomass for biofuels production. Fuel Processing Technology, 2010. **91**(1): p. 25-32.

25. Garcia, L.a., et al., Catalytic steam reforming of bio-oils for the production of hydrogen: effects of catalyst composition Applied Catalysis A: General, 2000. **201**: p. 225-239.

26. He, M., et al., Hydrogen-rich gas from catalytic steam gasification of municipal solid waste (MSW): Influence of catalyst and temperature on yield and product composition. International Journal of Hydrogen Energy, 2009. **34**(1): p. 195-203.

27. Meesuk, S., et al., The effects of temperature on product yields and composition of bio-oils in hydropyrolysis of rice husk using nickel-loaded brown coal char catalyst. Journal of Analytical and Applied Pyrolysis, 2012. **94**: p. 238-245.

28. Wu, C. and P.T. Williams, Investigation of Ni-Al, Ni-Mg-Al and Ni-Cu-Al catalyst for hydrogen production from pyrolysis–gasification of polypropylene. Applied Catalysis B: Environmental, 2009. **90**(1-2): p. 147-156.

29. Ago, H., et al., Gas analysis of the CVD process for high yield growth of carbon nanotubes over metal-supported catalysts. Carbon, 2006. **44**(14): p. 2912-2918.

30. Amama, P.B., et al., Role of Water in Super Growth of Single-Walled Carbon Nanotube Carpets. Nano Letters, 2009. **9**(1): p. 44-49.

31. Govindaraj, A., et al., An investigation of carbon nanotubes obtained from the decomposition of methane over reduced Mg1–xMxAl2O4 spinel catalysts. Journal of Materials Research, 1999. **14**(6): p. 2567-2576.

32. Hata, K., et al., Water-assisted highly efficient synthesis of impurity-free single-walled carbon nanotubes. Science, 2004. **306**(5700): p. 1362-4.

33. Kong, J., A.M. Cassell, and H. Dai, Chemical vapor deposition of methane for single-walled carbon nanotubes. Chemical Physics Letters, 1998. **292**: p. 567-574.

34. Takenaka, S., Formation of filamentous carbons over supported Fe catalysts through methane decomposition. Journal of Catalysis, 2004. **222**(2): p. 520-531.

35. Tan, S.-M., et al., Effects of FeOx, CoOx, and NiO catalysts and calcination temperatures on the synthesis of single-walled carbon nanotubes through chemical

vapor deposition of methane. Journal of Alloys and Compounds, 2009. **477**(1-2): p. 785-788.

36. Pol, V.G. and P. Thiyagarajan, Remediating plastic waste into carbon nanotubes. Journal of Environmental Monitoring, 2010. **12**(2): p. 455-459.

37. Wu, C., et al., Sustainable processing of waste plastics to produce high yield hydrogen rich synthesis gas and high quality carbon nanotubes. RSC Advances, 2012. **2**: p. 4045-4047.

38. Ahmed, I.I. and A.K. Gupta, Hydrogen production from polystyrene pyrolysis and gasification: Characteristics and kinetics. International Journal of Hydrogen Energy, 2009. **34**(15): p. 6253-6264.

39. Namioka, T., et al., Hydrogen-rich gas production from waste plastics by pyrolysis and low-temperature steam reforming over a ruthenium catalyst. Applied Energy, 2011. **88**(6): p. 2019-2026.

40. Tongamp, W., Q. Zhang, and F. Saito, Hydrogen generation from polyethylene by milling and heating with Ca(OH)2 and Ni(OH)2. International Journal of Hydrogen Energy, 2008. **33**(15): p. 4097-4103.

41. Wu, C. and P.T. Williams, Hydrogen production by steam gasification of polypropylene with various nickel catalysts. Applied Catalysis B: Environmental, 2009. **87**(3-4): p. 152-161.

42. Wu, C. and P.T. Williams, Pyrolysis–gasification of plastics, mixed plastics and real-world plastic waste with and without Ni–Mg–Al catalyst. Fuel, 2010. **89**(10): p. 3022-3032.

43. Alves, J.O., et al., Catalytic conversion of wastes from the bioethanol production into carbon nanomaterials. Applied Catalysis B: Environmental, 2011. **106**(3-4): p. 433-444.

44. Das, N., et al., The effect of feedstock and process conditions on the synthesis of high purity CNTs from aromatic hydrocarbons. Carbon, 2006. **44**(11): p. 2236-2245.

45. Juang, Z., On the kinetics of carbon nanotube growth by thermal CVD method. Diamond and Related Materials, 2004. **13**(11-12): p. 2140-2146.

46. Lee, C.J., et al., Temperature effect on the growth of carbon nanotubes using thermal chemical vapor deposition. Chemical Physics Letters, 2001. **343**: p. 33-38.

47. Jourdain, V. and C. Bichara, Current understanding of the growth of carbon nanotubes in catalytic chemical vapour deposition. Carbon, 2013. **58**: p. 2-39.

48. He, M., et al., Syngas production from catalytic gasification of waste polyethylene: Influence of temperature on gas yield and composition. International Journal of Hydrogen Energy, 2009. **34**(3): p. 1342-1348.

49. Wu, C. and P.T. Williams, Pyrolysis–gasification of post-consumer municipal solid plastic waste for hydrogen production. International Journal of Hydrogen Energy, 2010. **35**(3): p. 949-957.

50. Gallego, G.S., et al., Production of hydrogen and MWCNTs by methane decomposition over catalysts originated from LaNiO(3) perovskite. Catalysis Today, 2010. **149**(3-4): p. 365-371.

51. Bimbela, F., et al., Catalytic steam reforming of model compounds of biomass pyrolysis liquids in fixed bed: Acetol and n-butanol. Journal of Analytical and Applied Pyrolysis, 2009. **85**(1-2): p. 204-213.

52. Furusawa, T., et al., The evaluation of the stability of Ni/MgO catalysts for the gasification of lignin in supercritical water. Applied Catalysis A: General, 2007. **327**(2): p. 300-310.

53. Garcia, L., et al., Hydrogen Production by Steam Gasification of Biomass Using Ni-Al Coprecipitated Catalysts Promoted with Magnesium. Energy and Fuels, 2002. **16**: p. 1222-1230.

54. Jiang, Z.W., et al., Polypropylene as a carbon source for the synthesis of multi-walled carbon nanotubes via catalytic combustion. Carbon, 2007. **45**(2): p. 449-458.

55. Kong, Q.H. and J.H. Zhang, Synthesis of straight and helical carbon nanotubes from catalytic pyrolysis of polyethylene. Polymer Degradation and Stability, 2007. **92**(11): p. 2005-2010.

56. Tang, T., et al., Synthesis of multiwalled carbon nanotubes by catalytic combustion of polypropylene. Angew Chem Int Ed Engl, 2005. **44**(10): p. 1517-20.

57. Zhuo, C., et al., Synthesis of carbon nanotubes by sequential pyrolysis and combustion of polyethylene. Carbon, 2010. **48**(14): p. 4024-4034.

58. Yang, Z., et al., Coupled process of plastics pyrolysis and chemical vapor deposition for controllable synthesis of vertically aligned carbon nanotube arrays. Applied Physics A, 2010. **100**(2): p. 533-540.

59. Yen, Y.W., M.D. Huang, and F.J. Lin, Synthesize carbon nanotubes by a novel method using chemical vapor deposition-fluidized bed reactor from solid-stated polymers. Diamond and Related Materials, 2008. **17**(4-5): p. 567-570.

60. Wang, P., et al., Filamentous carbon prepared by the catalytic pyrolysis of CH4 on Ni/SiO2. Applied Catalysis A: General, 2002. **231**: p. 34-44.

61. Sengupta, J., et al., Effect of growth temperature on the CVD grown Fe filled multi-walled carbon nanotubes using a modified photoresist. Materials Research Bulletin, 2010. **45**(9): p. 1189-1193.

62. Malek Abbaslou, R.M., J. Soltan, and A.K. Dalai, The effects of carbon concentration in the precursor gas on the quality and quantity of carbon nanotubes synthesized by CVD method. Applied Catalysis A: General, 2010. **372**(2): p. 147-152.

63. Volder, M.F.L.D., et al., Carbon Nanotubes: Present and Future Commercial Applications. Science, 2013. **339**(6119): p. 535-539.

64. Allaouia, A., et al., Mechanical and electrical properties of a MWNT/epoxy composite. Composites Science and Technology, 2002. **62**: p. 1993-1998.

65. Montazeri, A., et al., Mechanical properties of multi-walled carbon nanotube/epoxy composites. Materials & Design, 2010. **31**(9): p. 4202-4208.

66. Rahaman, M.S., C.D. Vecitis, and M. Elimelech, Electrochemical carbon-nanotube filter performance toward virus removal and inactivation in the presence of natural organic matter. Environ Sci Technol, 2012. **46**(3): p. 1556-64.

67. Gao, G. and C.D. Vecitis, Electrochemical carbon nanotube filter oxidative performance as a function of surface chemistry. Environ Sci Technol, 2011. **45**(22): p. 9726-34.

68. Sotowa, C., et al., The reinforcing effect of combined carbon nanotubes and acetylene blacks on the positive electrode of lithium-ion batteries. ChemSusChem, 2008. **1**(11): p. 911-5.

69. Beigbeder, A., et al., Preparation and characterisation of silicone-based coatings filled with carbon nanotubes and natural sepiolite and their application as marine fouling-release coatings. Biofouling, 2008. **24**(4): p. 291-302.

70. Coleman, J.N., et al., High-Performace Nanotube-Reinforced Plastics: Understanding the Mechanism of Strength Increase. Advanced Functional Materials, 2004. **14**(8): p. 791-798.

71. Mohanty, P., M. Patel, and K.K. Pant, Hydrogen production from steam reforming of acetic acid over Cu-Zn supported calcium aluminate. Bioresour Technol, 2012. **123**: p. 558-65.

72. Rostrup-Nielsen, J.R., Steam Reforming Catalysts. 1975, Copenhagen: Danish Technical Press.